Contemporary Physics, 2000, volume 41, number 2, pages 61–78

Nanomagnets for sensors and data storage

K. J. KIRK

Miniaturized magnetic devices are ubiquitous in the hard disks of computers and in tape storage systems. Giant magnetoresistance was discovered as recently as 1988 but already sensors using the effect are being incorporated into read heads for the highest density hard disk systems. As a result of intensive research and development, storage density on hard disks has increased dramatically at a rate greater than 60% per year. At sub-micron and nano-scale dimensions the properties of magnetic devices are strongly affected by their size and shape in a complex way resulting from the interplay between different types of magnetic energy. In some cases this causes a deterioration in the performance of existing devices, however it has also enabled entirely new devices to be proposed. Arrays of nanomagnets could be used for ultra-high density storage on hard disks or for fast and dense, non-volatile, solid state memory. Storage applications are possible because hysteresis in the nanomagnets creates two oppositely magnetized states which are stable in zero applied field and can store binary data. Magnetic sensors based on giant magnetoresistance in layered magnetic structures are among the most sensitive available for operation at room temperature and above. This paper describes the physical properties of nanomagnets and their role in present and future applications.

1. Introduction

The magnetic data storage industry produced 140 million hard disk drives worth $27 000 million in 1998 [1]. Over the last 10 years the density of information stored on hard disks has increased dramatically, with growth rates now exceeding 60% per year. The rapid pace of technological development towards higher density data storage has led to an immense expansion of interest in magnetic materials, especially thin films, and has produced many spin-offs in research and technology for sensors, new types of memory, and even a new field of electronics based on the spin of the electron rather than its charge [2,3]. At the same time there has been a strong push towards miniaturization, in many cases the new devices will have dimensions deep in the nanometre regime, and will be made from magnetic films only a nanometre or so thick.

Research into magnetic materials has been particularly fruitful and new discoveries have been incorporated into commercial products at unprecedented speed. Traditionally, technologically useful magnetic materials fell into two classes [4]: so-called 'hard' magnetic materials which retain their magnetic state well and can therefore be used as permanent magnets or as the thin film coatings which store information on disks or tapes; and 'soft' magnetic materials which have a large change in their magnetic state for a small change in the external field and therefore are suitable as the active elements of sensors. As we shall see, this traditional distinction between hard and soft materials becomes less clear for magnets of small dimensions, where a nanomagnet made from a soft material may have ideal properties for data storage.

The key recent discovery in magnetic materials was giant magnetoresistance or GMR [5], a phenomenon in which a material undergoes a large change in resistance of typically 5–40% when an external field is applied. When there is a large GMR response to a small field very sensitive magnetic field sensors can be produced [6]. GMR sensors are already making inroads into magnetic data storage in the recording heads for hard disks. The GMR effect is most effectively exploited in layered

Author's address: Department of Physics and Astronomy, Department of Electronics and Electrical Engineering, University of Glasgow, Glasgow G12 8QQ, Scotland, UK.

Contemporary Physics ISSN 0010-7514 print/ISSN 1366-5812 online
http://www.tandf.co.uk/journals/tf/00107514.html

structures containing ferromagnetic and non-magnetic layers. For example, devices such as spin valves and spin tunnel junctions have been developed in which two magnetic layers are sandwiched with a spacer layer of either a non-magnetic metal or an insulator. There are exciting possibilities for GMR devices as small cheap and rugged sensors for use in navigation or mechanical systems, and for magnetic random access memory (MRAM), a type of fast and dense non-volatile memory which could eventually rival silicon DRAM [7,8].

Developments have also taken place in magnetically hard materials for hard disk coatings known as media. Up to four other metals are now alloyed with Co to produce a granular film with optimum properties for recording. Hard disk media in current production are magnetized in the plane of the disk, but materials are also being investigated which are magnetized perpendicular to the plane and could lead to higher density storage than for in-plane recording [9]. Perpendicularly magnetized media are already being used for magneto-optical recording. In magneto-optical technology the data is again stored in a magnetic coating on the disk but this time is written and read with the help of a laser [10,11]. The data storage density in magneto-optical systems is lower than on hard disk drives, since bit sizes are limited by the wavelength of the light, but they are nevertheless important for high density rewritable storage on removable disks. Near-field optical methods [12,13] could lead to higher density magneto-optical recording, with bit sizes far below the wavelength of the laser light, however they are still not expected to exceed the storage densities forecast for hard disks.

2. Looking at the effects of miniaturization

The trend in electronic devices is always towards miniaturization. It is only necessary to think of the increase in storage capacity of hard disks in personal computers over recent years to realize that Gbytes of data are being squeezed into a space which not long ago would have held only a few Mbytes. In this section I will discuss some of the effects on hard disk systems of miniaturizing their magnetic components to sub-micron dimensions, and describe how these effects are under investigation by magnetic imaging, magnetic measurements and computer simulation.

2.1. *Miniaturization issues in magnetic data storage*

The basic components of a hard disk system are the disk itself and the recording head. The most obvious way to increase the density of data storage is for each piece of data, or 'bit', to be stored in a smaller space on the disk. With miniaturization of the bits it follows that the other components of the system must be miniaturized too.

At the heart of an advanced recording head is the magnetoresistive sensor element. This is a small piece of thin film magnetic material which is a sensitive detector of magnetic field. Figure 1 shows a schematic diagram of the sensor reading a sequence of bits. The data is written by a tiny electromagnet, also built into the recording head, which magnetizes a small part of the disk to create each bit. Data is encoded as 'transitions' which are changes between two bits magnetized in opposite directions. The presence of a transition indicates a binary 1 and the absence of a transition (i.e. two adjacent bits written in the same direction) a binary 0. When data is being read, the vertical

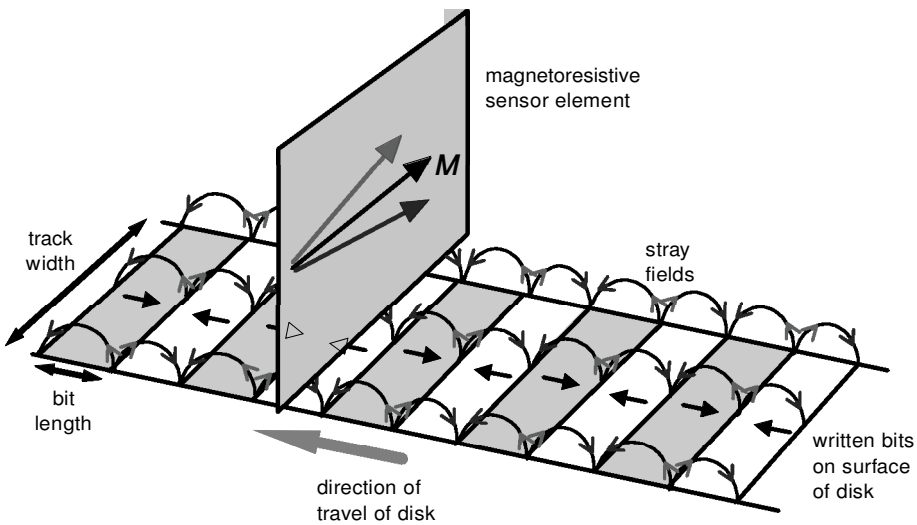

Figure 1. Magnetoresistive sensor element reading bits on a hard disk. The magnetization M of the sensor element changes its direction due to the stray magnetic field (pointing up or down) at the transitions between bits. An alternating pattern of bits, as shown here, would be read as a sequence of binary 1s.

magnetic field at the transition changes the orientation of the magnetization in the sensor, causing an increase or decrease in resistance.

The bits on a hard disk are arranged in concentric circular tracks. Therefore, to increase the density of stored information, the bit length (the distance between transitions) and the track width both need to shrink. Recent milestones for storage density in demonstration systems are 16 Gb in^{-2}, from drive manufacturer Seagate Technology in March 1999 [14] and 20.7 Gb in^{-2} from the Read-Rite Corporation in May 1999. For the 20.7 Gbit in^{-2} record, the bits were 55 nm wide, there were 1700 tracks per millimetre, and the recording head was travelling only 15 nm from the disk. Seagate recently announced (June 1999) a dramatic increase in track density to over 4100 tracks per millimetre by improving the accuracy with which their recording heads could follow narrower tracks.

Reducing the sizes of the magnetic components of the system into the micron and sub-micron regime does, however, begin to have adverse effects on their performance. One major issue arises from the miniaturization of the bits written on the disk: for small bits the finite size of the grains in the media starts to become noticeable, leading to indistinct transitions (figure 2). It is also important to consider the effect of miniaturization on the sensor element in the read head which faces the twin requirements of smaller physical dimensions and increased sensitivity in order to read smaller bits. Despite a number of difficult practical problems to be solved along the way, the magnetic data storage industry predicts reaching 100 Gbit in^{-2} using improved versions of today's technology. The development of new techniques and new devices to combat the problems and continue the trend of increasing storage density are topics of current research and some of them will be discussed later in this paper.

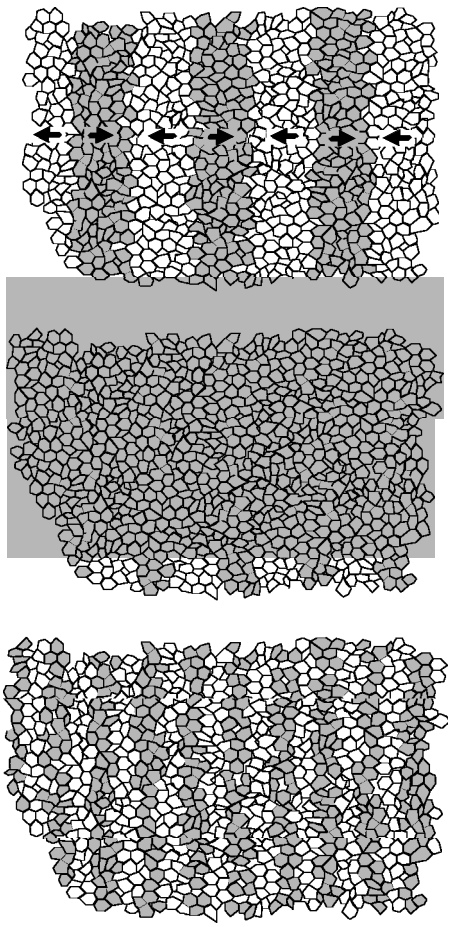

Figure 2. The effect of reducing the size of the bits in a thin film granular coating on a hard disk. As the bit size approaches the grain size, the transitions become indistinct leading to a rather noisy signal. Grain size in the Co alloy films currently used is typically 12–15 nm, compared with a bit length of $\leqslant$ 55 nm.

2.2. *Nanomagnetic investigations*

To predict and improve the properties of miniaturized magnetic systems we need to understand the nanomagnets which are their active components. The properties of physically interesting and technologically relevant magnetic structures and devices are therefore under investigation both by experiments and by simulation techniques [15]. Two important basic questions are: what is the magnetic state of the nanomagnets at zero field, and how does this change when a magnetic field is applied? To answer these questions, individual nanomagnets and arrays have been fabricated using high resolution techniques including electron beam lithography, X-ray lithography [16], laser interferometry [17], self-assembly [18], electro-deposition [19], and various types of nano- imprinting [20,21]. Direct visualization of the magnetic behaviour is possible using magnetic imaging techniques [22], the highest resolution being available using the transmission electron microscope (TEM) [23,24] and magnetic force microscopy (MFM) [25,26,27,28]. Other types of magnetic measurement do not allow direct observation of the magnetic processes but enable the properties of the nanomagnets to be deduced from results from an ensemble of elements [29] or from individual particles [30–33].

At Glasgow University we specialize in Lorentz imaging in the TEM. There are several imaging modes in all of which magnetic contrast is generated by the deflection of the electrons by the Lorentz force as they pass through a magnetic sample [23]. We have studied thin film elements in the size range 4 μm to 25 nm, fabricated mainly by electron beam lithography [34,35]. Magnetic information can be obtained down to 2–20 nm resolution. Magnetic domain patterns can be clearly seen and magnetization processes can be observed in real time. Information on the physical microstructure and the chemical composition is also

available from the TEM and can be correlated with the observed magnetic microstructure to give a complete picture of how the magnetic properties are affected by defects, grain size and irregularities.

Advances in computer modelling combined with improvements in high resolution lithography and imaging over the last ten years mean that experimental and simulated results can now be compared for nanomagnetic systems. Theoretical work on nanomagnets has helped to clarify some details of the magnetic processes, explore the parameters required for improved devices, and extend our understanding into regimes which are difficult to access experimentally, such as extremely fast time-scales and very tiny elements.

3. Properties of small magnetic elements

In this paper I shall concentrate on the properties of thin film elements of micro-polycrystalline soft magnetic material such as $Ni_{80}Fe_{20}$ (NiFe) and pure Co. These sorts of magnetic films, patterned into elements with micron and sub-micron dimensions, have proved to be versatile for a wide range of applications in sensors, memory elements and data storage. Their behaviour is strongly affected by their shape and size in the micron and nano-scale regime, as we shall see.

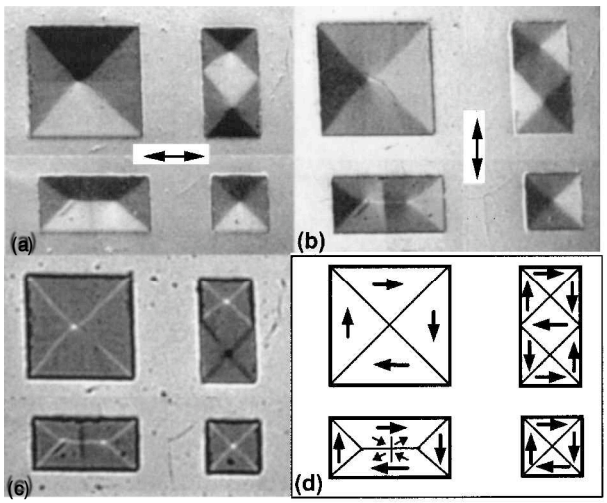

Figure 3. Magnetic domains in NiFe elements observed by two different Lorentz imaging modes in the transmission electron microscope. In Foucault mode, (*a*) and (*b*), we can see the direction of magnetization in the domains (white and black indicate opposite magnetization directions parallel to the double headed arrows). In Fresnel mode, (*c*), the domain walls are visible. These elements have a flux closure domain structure in which the magnetization forms closed loops as shown in the schematic diagram (*d*). The dimensions of the elements are 2 μm $\times$ 2 μm, 1 μm $\times$ 2 μm, 2 μm $\times$ 1 μm and 1 μm $\times$ 1 μm. Film thickness is 20 nm.

3.1. *Magnetic domain structures*

We will now begin to look at the magnetization distribution within a thin film element of magnetic material. $\mathbf{M}(\mathbf{r})$ is the magnetization vector at each point, where $|\mathbf{M}| = M_s$ is the saturation magnetization. M_s is a characteristic of the material and has a constant value in a sample of uniform composition. It is the orientation of $\mathbf{M}$ which varies throughout the sample giving rise to the huge variety of domain patterns observed.

Figure 3 shows magnetic images of square and rectangular elements of NiFe film, 20 nm thick. The elements are shown in plan view in the TEM. They are magnetized in the plane of the film with magnetization distributions shown in the schematic diagram, figure 3 (*d*). In figures 3 (*a*) and (*b*) (Foucault mode) the light and dark shading shows the magnetic domains, which are areas of more or less constant magnetization. In each case, white and black indicate opposite magnetization directions parallel to the double-headed arrow, while domains magnetized perpendicular to the arrow appear grey. Using another imaging mode, known as the Fresnel mode, figure 3 (*c*) shows the domain walls which form the boundaries between the domains. At a domain wall the magnetization rotates, usually by 90° or 180°, from one domain to the next. These elements have 'flux closure' domain patterns in which the magnetization in the elements forms a closed loop.

The different domain patterns result from the competing magnetic influences in micron and sub-micron sized elements. The exchange interaction, a consequence of the quantum mechanical origin of magnetism, attempts to have the whole of the element magnetized the same way. To minimize the magnetostatic energy, however, the magnetization would like to split into many domains, to form closed magnetic loops and minimize the stray fields. The magneto-crystalline anisotropy, meanwhile, would prefer the magnetization to lie along certain crystal axes in the material, or, in a polycrystalline material, along a preferred direction (or *easy axis*) sometimes created by growing the film in an applied field. In addition, the element experiences the magnetizing effect from any external magnetic field.

In a nanomagnet of soft magnetic material at zero field, the dominant effects are from the competition between the exchange energy and the magnetostatic energy. When the magneto-crystalline anisotropy is very low, or when it averages to zero in a polycrystalline material, the magnetization has no preferred directions and is quite happy to follow the edges of the element, as was clearly seen in the flux closure domain patterns in figure 3. A different type of domain structure is seen in more elongated rectangles in figure 4. These elements take up a 'near single domain' state with uniform magnetization in most of the element, except for small domains at the ends where the magnetization

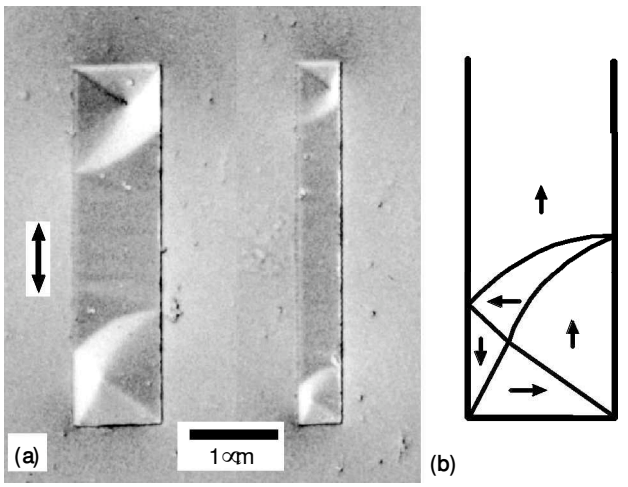

Figure 4. Domain structure in elongated rectangles 4 μm $\times$ 1 μm and 4 μm $\times$ 0.5 μm, made from a NiFe film 26 nm thick: (*a*) magnetic image and (*b*) schematic. Complete flux closure is not possible in these elements so they become predominantly magnetized along their length. Vortex-type domains commonly form at the ends. Stray fields can be seen outside the elements as dark shading at the ends and lighter shading at the sides.

loops round to achieve partial flux closure, thereby reducing, but not eliminating, the stray field. For complete flux closure in these elements it would be necessary to have either a very long central domain wall running parallel to the long axis or a high density of shorter walls running transversely. Neither of these scenarios would be favoured by the exchange interaction since they would entail deviation from uniform magnetization over a large part of the element.

We have seen that domain walls exist at the boundaries between domains of different magnetization direction. Inside the wall the magnetization must somehow swing round from one direction to another. In fact there are a number of wall types with characteristic width and properties [36]. In soft thin films Néel walls predominate in which the magnetization vector stays parallel to the plane of the film while it gradually rotates from one direction to the next. In a magnetic film with low anisotropy, such as NiFe, this will cost very little magnetostatic or magneto-crystalline energy. To minimize the energy, the exchange interaction tries to enforce a very slow change in the magnetization direction across the wall. Therefore Néel walls are very wide, about 200 nm in a continuous film. For many years it was tempting to believe that walls could not form inside nanomagnets narrower than a standard wall width—therefore they would be truly single domain. However it has been clearly shown by high resolution magnetic imaging that domain walls can indeed be accommodated. The walls themselves will no longer be simple Néel walls but will have a more complicated structure, with their detailed form depending on the thickness of the film [37].

The concept of shape anisotropy is particularly important in small elements. This is the tendency for the magnetization to align along the length of the element, creating an easy axis defined by the shape. Shape anisotropy minimizes the magnetostatic energy by keeping the magnetization parallel to the long edges of an element. More stray field, and therefore more stray field energy, is generated if the magnetization meets head-on the long edges of a rectangle rather than the shorter ones. For the same reason, the magnetization in a continuous thin film usually lies in the plane of the film rather than perpendicular to it.

3.2. *Switching fields and switching mechanisms*

It is quite clear, then, that the shape of a nanomagnet has a very strong effect on its domain patterns. These in turn affect its magnetic properties, such as its switching field—the field required to switch the magnetization from one direction to the opposite direction. For example, elongated rectangular elements (as seen in figure 4) have been found to have certain characteristic properties. The magnetization aligns along the long axis and a single domain occupies most of the element: therefore there are two stable magnetic states. The coercivity of an element can easily be more than 100 times the coercivity of an unpatterned soft magnetic film of the same material. The element width has a strong effect on the applied field needed to switch between the two stable states. Figure 5 shows how the switching field of Co and NiFe elements of a similar thickness, applied parallel to the long axis of the elements, increases as the width decreases.

It is also important to know the mechanism by which switching occurs. In general, switching will proceed by some combination of three basic mechanisms: rotation of the magnetization within a domain, growth of existing domains, or formation of new domains. For example, observations in the TEM on elongated rectangular nanomagnets made from NiFe and Co have shown that switching starts by growth of the flux closure domains at the ends [38]. Above an aspect ratio (length/width) of about 4 : 1 there is no effect from the element's length on its switching field. This tells us something else about the switching mechanism in these elongated elements—switching occurs independently from one end or the other with no interaction between the end domains.

Information on the switching fields and mechanisms gives a good indication of how the geometry of a nanomagnet could be modified in order to alter its magnetic properties. In the case of elongated elements the switching field is more than doubled if the end

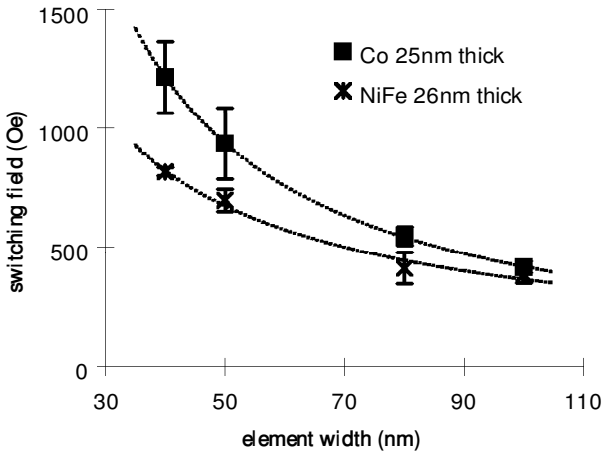

Figure 5. Increase of switching field of rectangular nanomagnets of NiFe and Co as their width is decreased. The aspect ratio of these elements (length/width) was between 3.75 and 10 but in this range it had little effect on the switching field.

domains are suppressed by changing the ends of the element from a rectangular to a pointed shape [39]. Because they have two stable magnetization states, elongated elements are suitable for data storage applications. The two opposite states can be used to store binary data and the high switching field gives the elements stability to retain the data against external magnetic influences.

3.3. *Predicting the behaviour of nanomagnets*

3.3.1. *Stable states.* For a long time attempts have been made to predict the behaviour of small magnetic elements, to enhance our knowledge of the physics of magnetism at small dimensions and as a tool for the development of new magnetic devices and systems. Therefore micromagnetic models have been produced which consider the influences acting on the system and show the probable resulting domain patterns.

An effective method to predict stable magnetization configurations, the ones seen in real systems, is to calculate the energy minima of the system using the magnetic Gibbs free energy. The magnetic Gibbs free energy is the sum of the relevant magnetic energy terms, generally including the exchange energy, the magnetostatic energy, the magneto-crystalline anisotropy energy and the potential energy of the system in the external applied field. Stable states are therefore local minima on a complex energy surface. During a magnetization cycle, the system follows a route over this energy surface, which will be distorted by changes in the applied field. Magnetic hysteresis arises because in general the same route cannot be retraced on the reverse path.

Equations for the most important terms of the magnetic Gibbs free energy are given below. In each case the energy is integrated over the volume, V, of the system. The total free energy, E_{tot}, is the sum of these terms. At a stable state, E_{tot} has a local minimum, subject to the constraint that $|\mathbf{M}|$ remains constant throughout the system.

Exchange energy

$$E_{\mathrm{ex}} = \int_V A \sum_{\mathrm{i}=1}^{3} (\nabla \beta_{\mathrm{i}})^2 \, \mathrm{d}V , \tag{1}$$

Magnetostatic energy

$$E_{\mathrm{mag}} = -\tfrac{1}{2} \int_V (\mathbf{H}_{\mathrm{d}} \cdot \mu_0 \mathbf{M}) \, \mathrm{d}V , \tag{2}$$

Magneto-crystalline anisotropy energy

$$E_{\mathrm{an}} = -\int_V K_{\mathrm{u}} (\mathbf{u} \cdot \beta)^2 \, \mathrm{d}V , \tag{3}$$

Magnetic potential energy

$$E_{\mathrm{pot}} = -\int_V (\mathbf{H}_{\mathrm{app}} \cdot \mu_0 \mathbf{M}) \, \mathrm{d}V . \tag{4}$$

Here $\mathbf{M}$ is the magnetization vector and β is the direction cosine of the magnetization vector ($\mathbf{M} = M_{\mathrm{s}} \beta$). A is the exchange constant [40] and μ_0 is the permeability of free space. $\mathbf{H}_{\mathrm{app}}$ is the external applied field, $\mathbf{H}_{\mathrm{d}}$ is the self-demagnetizing field, K_{u} is the uniaxial anisotropy constant of the material and $\mathbf{u}$ is the anisotropy direction.

Looking at the equations, we can get an idea of what factors determine the magnitude of these terms. Exchange energy (1) depends on the rate of change in angle of the magnetization vector from one point to the next. If the angle of $\mathbf{M}$ is steeply varying, as it could be in a domain wall, the exchange energy will be large. The factor A, the exchange constant, is analogous to an elastic constant for the magnetic material. The magnetostatic energy contribution (2) to the total depends strongly on the sample geometry, via the demagnetizing field. This can be difficult to determine precisely since the magnetization configuration inside the sample is affected by the stray fields it produces itself. Some simple cases and useful approximations are described below. The magneto-crystalline energy (3) lowers the total energy if $\mathbf{M}$ lies along $\mathbf{u}$, the easy axis of the material. In NiFe K_{u} is small so this energy contribution may be negligible compared to the other terms, especially for nanomagnets. The magnetic potential energy (4) is generated by applying an external field. This term will most effectively minimize the total energy if the magnetization in the sample aligns in the same direction as the applied field.

The demagnetizing field $\mathbf{H}_d$ depends on the geometry of the system via a demagnetizing factor, N, defined by

$$\mathrm{H}_d = -N\mathbf{M} . \quad (5)$$

A simplification frequently made for a thin film element is to approximate it by a uniformly magnetized, very oblate, ellipsoid with its two major axes the same as the length and width of the element [41]. The two in-plane dimensions a and b must be much larger than the thickness c. The demagnetizing factor when the sample is magnetized along the long axis, a, in the plane of the film is then

$$N_a = \frac{\pi}{4}\frac{c}{a}\left[1 - \frac{1}{4}\frac{a-b}{a} - \frac{3}{16}\left(\frac{a-b}{a}\right)^2\right] \quad (6)$$

and for the sample magnetized along the short axis, b, also in the plane, is

$$N_b = \frac{\pi}{4}\frac{c}{a}\left[1 + \frac{5}{4}\frac{a-b}{a} - \frac{21}{16}\left(\frac{a-b}{a}\right)^2\right]. \quad (7)$$

The out-of-plane demagnetizing factor N_c is related to N_a and N_b by

$$N_a + N_b + N_c = 1 . \quad (8)$$

N_c should be ~ 1 if the assumption of a very oblate ellipsoid is correct. For an element measuring 1 μm $\times$ 200 nm $\times$ 25 nm, the demagnetizing factors in the plane of the film are $N_a = 0.013$ along the length and $N_b = 0.023$ across the width. For out-of-plane magnetization, $N_c = 0.96$. With no external field and negligible magneto-crystalline anisotropy, the magnetization will orientate in the direction giving the smallest demagnetizing field in (5), i.e. along the long axis a. This is the origin of shape anisotropy. Clearly if the in-plane dimensions of a nanomagnet are very small they could become comparable to the film thickness and the assumption of a very oblate ellipsoid ($a > b >> c$) will no longer be valid. If a different approximation cannot be used, numerical methods are then needed to calculate the demagnetizing field.

A very useful simplification of the total energy of a magnetic element is given by the Stoner–Wohlfarth equation, which can be used to predict switching fields and hysteresis loops of a uniformly magnetized magnetic sample. The total Stoner–Wohlfarth energy of the element is

$$E_{\mathrm{SW}} = K\sin^2\varphi - H_{\mathrm{easy}}M_s\cos\varphi - H_{\mathrm{hard}}M_s\sin\varphi , \quad (9)$$

where K is the uniaxial anisotropy constant, φ is the angle between $\mathbf{M}$ in the element and the easy axis, and H_{easy} and H_{hard} are the applied field components, parallel and perpendicular to the easy axis, in the plane of the element. For the Stoner–Wohlfarth equation to be applicable the magnetization in the element must be uniform throughout and must be assumed to rotate coherently under the influence of the applied field. There must be a single easy axis (uniaxial anisotropy). The anisotropy constant K can either refer to the magneto-crystalline anisotropy, with constant K_u, or the shape anisotropy using the stray field energy constant K_d,

$$K_d = \frac{\mu_0 M_s^2}{2}, \quad (10)$$

whichever dominates in the element in question.

Using (9) the total energy *for each orientation of* $\mathbf{M}$ can be found for different values of applied field. Therefore the stable directions of magnetization in the element can be identified as the orientations of $\mathbf{M}$ giving energy minima. When changing the external field an energy minimum may disappear, so if the system was previously stable in that minimum it must go to a new, lower, minimum. If the applied magnetic field is opposite to the initial magnetization direction, complete switching may occur. The Stoner–Wohlfarth assumption that the system switches by coherent rotation of $\mathbf{M}$ is necessary so that uniform magnetization is preserved at all times. However we know that in real systems it is common for the magnetization in an element to change by means of domain processes, so the Stoner–Wohlfarth value for the switching field will be an overestimate [42]. Nevertheless it is useful as an upper bound to the switching field, and to predict some general trends.

3.3.2. *Dynamic solutions.* Even when using energy models more complex than the Stoner–Wohlfarth picture, there is ample experimental evidence that modelling magnetization reversal by considering only the stable states at the energy minima is not completely reliable. For example, some energy states may have very similar energy, such as in the 2 μm $\times$ 1 μm and 1 μm $\times$ 2 μm elements in figure 3, which makes the end result very sensitive to the exact path by which reversal takes place [43]. Therefore dynamic solutions can be used to determine the magnetic state of an element during a particular field cycle. In this picture, the system stays in an energy minimum until the minimum disappears, as in the static methods, but then follows the dynamic equations to reach a new stable state.

Another limitation of static energy minimization methods for micromagnetic modelling is that they do not take into account the speed of reversal. With increasingly fast systems being used for data storage it becomes necessary to investigate high frequency processes where a quasi-static approach is inadequate and dynamic modelling is vital.

Most dynamic models work by taking $\mathbf{H}_{\mathrm{eff}}$ as the effective field acting on a particular point in the magnetic sample. Equilibrium is reached when

$$\mathbf{H}_{\mathrm{eff}} = -\frac{\partial E_{\mathrm{tot}}}{\partial \mathbf{M}}, \quad (11)$$

so the system is at a local minimum in energy, and

$$\mathbf{M} \times \mathbf{H}_{\mathrm{eff}} = 0, \quad (12)$$

so the torque on the magnetization is zero. When a new external field is applied, the magnetization precesses around the field direction according to

$$\frac{1}{\gamma}\frac{\partial \mathbf{M}}{\partial t} = \mathbf{M} \times \mathbf{H}_{\text{eff}}, \tag{13}$$

where γ is the gyromagnetic ratio for an electron. Energy dissipation is brought into the equations via a damping term, α, which is found from ferromagnetic resonance experiments and is usually in the range 0.01–1. α represents critical damping. When damping is included E_{tot} decreases over time and $\mathbf{M}$ rotates towards $\mathbf{H}_{\text{eff}}$ until parallel so the torque is again zero. For full equations incorporating the damping term, see [43].

Both dynamic micromagnetic simulations and those based on energy minimization require numerical techniques on high speed computers to calculate the demagnetizing field of the system and perform the minimization or integrate the equation of motion for $\mathbf{M}$. The first step in this kind of modelling is to discretize the magnetic element into smaller volumes with edge size of the order of the exchange length, ℓ_{ex},

$$\ell_{\text{ex}} = \left(\frac{A}{M_{\text{s}}^2}\right)^{1/2}. \tag{14}$$

Within each discretization volume, the magnetization can, justifiably, be assumed to be uniform so an equation can be written for its energy, E_{tot}, in the applied field. As ℓ_{ex} is just a few nanometres it becomes clear why nano-scale magnetic elements are easier and quicker to model than larger ones where discretization produces many thousands of equations to be solved.

4. Applications of nanomagnetics in new technology

Nanomagnetic systems are an important part of today's technology and have potential for new devices for the future. In this section I will discuss three main applications of nanomagnets: proposed patterned media for hard disks; miniature magnetic sensors employing the GMR effect, currently used in advanced recording heads; and magnetic memory cells or MRAM which are being developed for fast and dense solid state memory.

4.1. *Patterned media for hard disks*

The trend towards hard disks with a greater storage density still seems unstoppable and the increase in storage density is actually accelerating rather than slowing down. However effects associated with the finite grain size of magnetic alloys used for storage could prevent indefinite miniaturization [44]. To reach ultra-high storage densities, a new type of storage media has been proposed made from a closely-packed array of nanomagnets patterned onto a hard disk [45].

4.1.1. *The superparamagnetic limit.* Conventional hard disk media are continuous films of granular Co alloys. Writing data on the disk involves aligning the magnetization of a small area of the media. The films used for media are specially designed so that the grains are 'exchange-decoupled'. This means that each grain reverses individually and very localized areas of the disk can be written, enabling the bits to be very small and well defined. Intergranular exchange coupling is suppressed by adding non-magnetic ingredients, in particular Cr, which segregate to the grain boundaries breaking the ferromagnetic connection between the grains. At the same time the signal-to-noise ratio and the coercivity of the medium must be optimized. Magnetostatic interactions between the grains will still occur and each grain needs to have a high coercivity in order to withstand the magnetostatic influence of its neighbours.

In the quest for smaller bits, the size of the grains has been steadily reduced. Smaller grains help avoid uneven transitions between bits and ensure a minimum number of grains per bit to limit statistical noise. However there is a danger in continuing to reduce the grain size of the media. If the grains are too small, their magnetic energy becomes comparable to their thermal energy and their magnetization direction can switch freely, like the atoms in a paramagnetic material. Of course, if individual grains on a hard disk are susceptible to thermal switching at room temperature then the stored information will rapidly disappear. The limit on grain size is known as the superparamagnetic limit and has been predicted to be around 10 nm using current media [46].

Smaller grains can only be used if their switching field is increased. This is in fact possible by altering the composition of the Co alloy. Higher coercivity, around 3500 Oe, has been achieved by moving to four and five component Co alloys incorporating Ta and Pt to increase the magnetocrystalline anisotropy of the grains [47,48]. Even greater coercivity, up to 10 000 Oe, would be possible if hard magnet materials such as SmCo or NdFeB were used as media. With this coercivity, grain sizes could in theory be reduced to 2.5 nm. However this would put impossible demands on the *write heads* available today, which are limited to write fields of 5000 Oe. This is a key problem facing the hard disk industry in its plans for the future. One solution could be thermally assisted writing, where the coercivity of the media would be weakened locally using a laser pulse to make it easier to magnetize.

4.1.2. *Requirements for patterned media.* Higher storage densities, in the 100–500 Gbit in^{-2} range, could be reached using patterned media. Instead of a bit being a collection of exchange-decoupled grains, it would be an

individual nanomagnet made from an exchange-coupled film like NiFe. The media would then consist of an array of nanomagnet bits, physically isolated from their neighbours and able to be switched independently. The strong intergranular exchange coupling within the film ensures that all the grains in a bit switch at once. Depending on the material, a nanomagnet bit could be thermally stable down to around 10–20 nm in size, leading to ultra-high storage densities. At the same time the switching fields would be of moderate size, thus reducing the demands on the write head. Sharp transitions between bits are guaranteed by lithographic patterning. The signal-to-noise requirement to have many grains per bit no longer applies—therefore extremely small grain sizes are not required.

To store one bit of data, each nanomagnet must have two distinct magnetization states. This is easily achieved using elongated elements of soft magnetic materials with uniaxial shape anisotropy. The bits could be oriented either in the plane of the disk or perpendicular to it. Suitable candidates (shown in figure 6) are (a) bars patterned in the plane of the disk, (b) pillars with their long axis vertical [49], or (c) cones. A perpendicular configuration allows the nanomagnets to be packed more densely, whilst an in-plane configuration would enable more conventional reading and writing technology to be used.

Figure 7 shows an image from the transmission electron microscope showing nanomagnet bars of Co film, with nominal dimensions 200 nm × 40 nm and thickness 25 nm, fabricated at Glasgow. With one bit stored per element, this would correspond to a storage density of 27 Gb in^{-2}. Magnetic imaging shows the Co nanomagnets to be magnetized along their length. Their average switching field is 1200 Oe. The sequence of magnetic images in figure 8 show how an array of NiFe nanomagnets of the same size reverse their magnetization in an applied field. These have a lower average switching field of around 800 Oe. Researchers elsewhere have shown that it is possible to write 'data' to nanomagnet arrays by reversing the magnetization of individual elements, usually using the localized field from the probe of a magnetic force microscope [50]. It has also been possible to detect the magnetization direction of perpendicular Ni pillars using an ordinary read head scanned across an array [51].

The packing density of an array is limited by magnetostatic interactions between adjacent elements. Interactions have the effect of lowering or raising the switching field compared to what would be expected for an isolated element. Depending on the magnetization state and position of the neighbours, demagnetizing or magnetizing effects will occur. For example we have seen that the distribution of switching fields was widened in an array of elements arranged side by side when their spacing was made the same as their width or smaller [39]. It is important that the effect of interactions does not cause an element to switch at too low a field so it could be accidentally overwritten during writing of its neighbours, or at too high

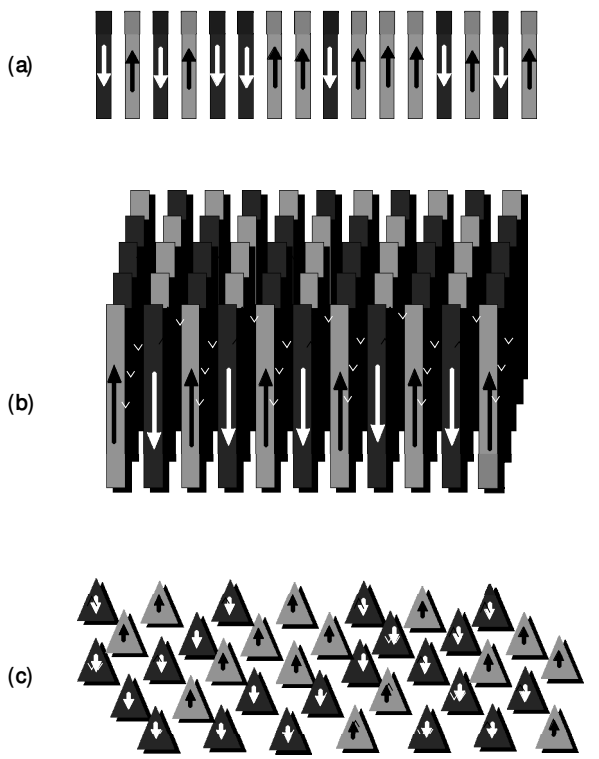

Figure 6. Possibilities for patterned media: (*a*) bars in the plane of the disk, (*b*) perpendicular pillars and (*c*) cones. Nanomagnets for data storage on hard disks must have two distinct magnetization states. This can be achieved using the special shape-controlled properties of elongated elements.

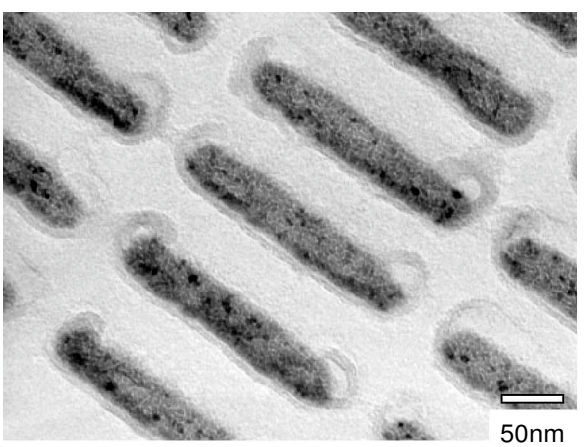

Figure 7. Co nanomagnet bars 200 nm × 40 nm, 25 nm thick, fabricated by electron-beam lithography and viewed in the transmission electron microscope. With one bit stored per element this would correspond to a storage density of 27 Gbit in^{-2}.

a field so it would fail to be written by the recording head. To avoid these problems, the size, shape, and aspect ratio of the elements in the nanomagnet array must be tailored for optimum density and performance.

4.1.3. *Practical issues for mass production.* If patterned media are to be taken up for commercial hard disk systems, cost effective methods of mass production of magnetic nano-elements must be developed. Most of the fabrication methods used in research on nanomagnets would not be suitable. Electron beam lithography is highly versatile and can produce very small elements, but is a rather slow serial process. Laser interference lithography can be used to cover large areas at once but is restricted to regular rectangular arrays [52]. More promising pattern transfer techniques are nano-imprint lithography [53] or embossing [54] which use electron beam fabricated master moulds, or some kinds of 'soft lithography' in which flexible moulds are used [55]. Ion beam modification of a continuous film would have the benefit of retaining a smooth and flat recording surface [56]. In recent experiments using ion beam bombardment, magnetically softer areas with in-plane magnetization were created in perpendicularly magnetized CoPt multilayers by mixing the layers.

New recording head designs will also be needed for patterned media, particularly if the stray field from the nanomagnet bars or pillars is in a different direction from that in current systems. It will also be necessary to synchronize writing the data with the position of the bits. This will involve greater control of the head position and more servo information, describing the exact position of the elements, to be written on the disk. If the bits are too small to read and write using conventional recording heads, alternative techniques will be needed to access the data [57].

4.2. *GMR sensors*

Sensors based on GMR are an exciting class of device with applications in mechanical and navigational systems, as well as their major use in read heads for hard disks. The origin of the GMR effect is the difference in scattering of electrons of opposite spin (up or down) as they pass through a ferromagnetic material [3,58]. For a particular orientation of magnetization in the material this spin-dependent scattering will lead to one type of electron experiencing a higher resistivity than the other.

4.2.1. *The GMR effect.* Layered magnetic structures have proved most useful for GMR devices. Spin-dependent scattering occurs in the magnetic layers and at the interfaces. For example, a simple GMR sensor could consist of two magnetic layers which can have their magnetization oriented either parallel or antiparallel to each other. When the two layers are magnetized antiparallel, the spin-up and spin-down electrons will be scattered equally. However, when the layers are magnetized parallel, the spin-dependent scattering results in a lower resistivity for one type of electron and a higher resistivity for the other type. The spin-up and spin-down electrons act as parallel conduction channels, so lowering the resistivity for one type

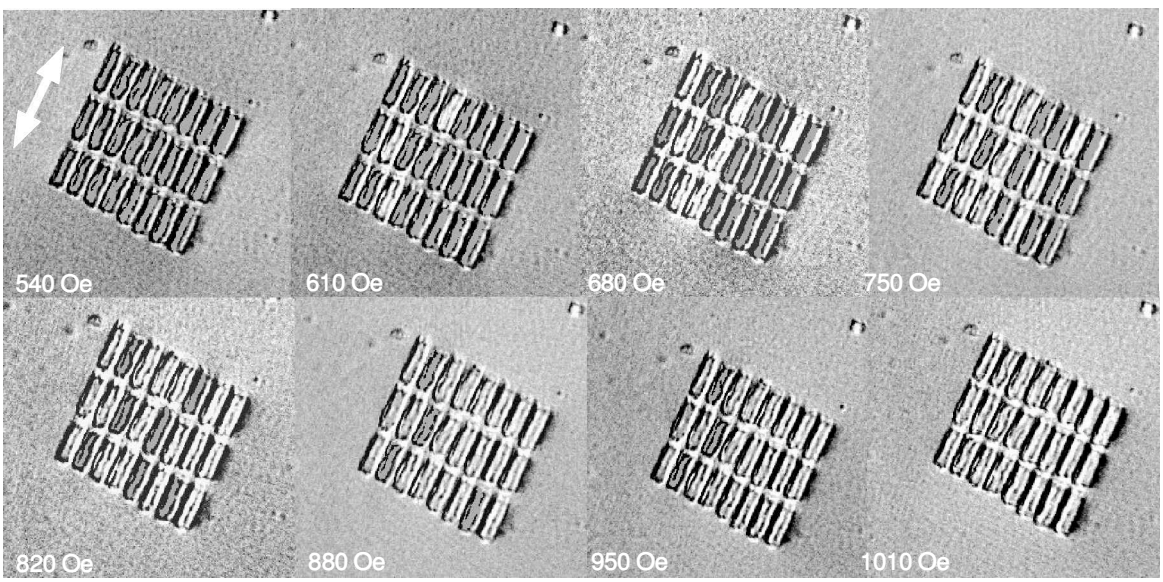

Figure 8. Magnetization sequence for an array of 200 nm × 40 nm NiFe nanomagnets. Light and dark colours indicate opposite magnetization directions, parallel to the arrow. The field was applied parallel to the long axis of the elements, inside the transmission electron microscope.

results in a lower resistance for the structure as a whole.

The crucial feature for obtaining the GMR effect is that an applied field should change the *relative* orientation of magnetization in the layers. A two layer sensor could be designed so the field to be detected rotates the magnetization in one layer from antiparallel to parallel orientation with respect to the other layer. This would give a measurable decrease in resistance. The important parameters of a GMR structure are the maximum fractional change in resistance, $\Delta R/R$, and the saturation field required to achieve the full range of response. A very sensitive low field sensor would have a large $\Delta R/R$ and a small saturation field.

Multilayers, spin valves and spin tunnel junctions, as described below, have all been investigated for use in commercial sensors. This invariably means they will be patterned into micron and sub-micron sized elements. Experiments have shown that the suitability of small GMR elements for sensors depends strongly on their dimensions as a result of shape anisotropy and stray field effects.

4.2.2. *Multilayers, spin valves and spin tunnel junctions.* Giant magnetoresistance was first discovered in Fe–Cr superlattices with thin non-magnetic Cr layers, less than 2 nm thick, separating slightly thicker Fe layers [5]. The effect was subsequently investigated in other multilayers of magnetic and non-magnetic metals, for example and Co–Cu [59] and Ni–Cu [60]. Parallel magnetization in the layers produces a low resistance state and antiparallel magnetization gives a high resistance state, as indicated in figure 9 (*a*). In zero field the magnetic layers are aligned in the antiparallel high resistance state by antiferromagnetic coupling. In an applied field the layers are forced into the parallel alignment, pointing in the applied field direction, giving the low resistance state. Multilayers comprising up to 30 magnetic–non-magnetic bilayers can have a rather large $\Delta R/R$ (up to 100%) but require a field of several hundred oersted (Oe) to overcome the antiferromagnetic coupling and saturate them in the low resistance state. Lower values for the saturation field have been achieved in modified structures, for example by using thicker non-magnetic layers, but at a cost of a somewhat lower magnetoresistance ratio. Multilayers therefore cannot be used as detectors of very small fields, however they are suitable for larger field applications and are under investigation for position sensors in mechanical systems [61].

A more sensitive response to an applied field is possible using a spin valve structure (figure 9 (*b*)). Spin valves, discovered in 1991 [62], have two soft magnetic layers, originally both NiFe, separated by a metallic spacer layer, usually Cu. There is no antiferromagnetic coupling between the layers. The GMR effect is generated by having a 'pinned' layer, held rigidly to a fixed magnetization

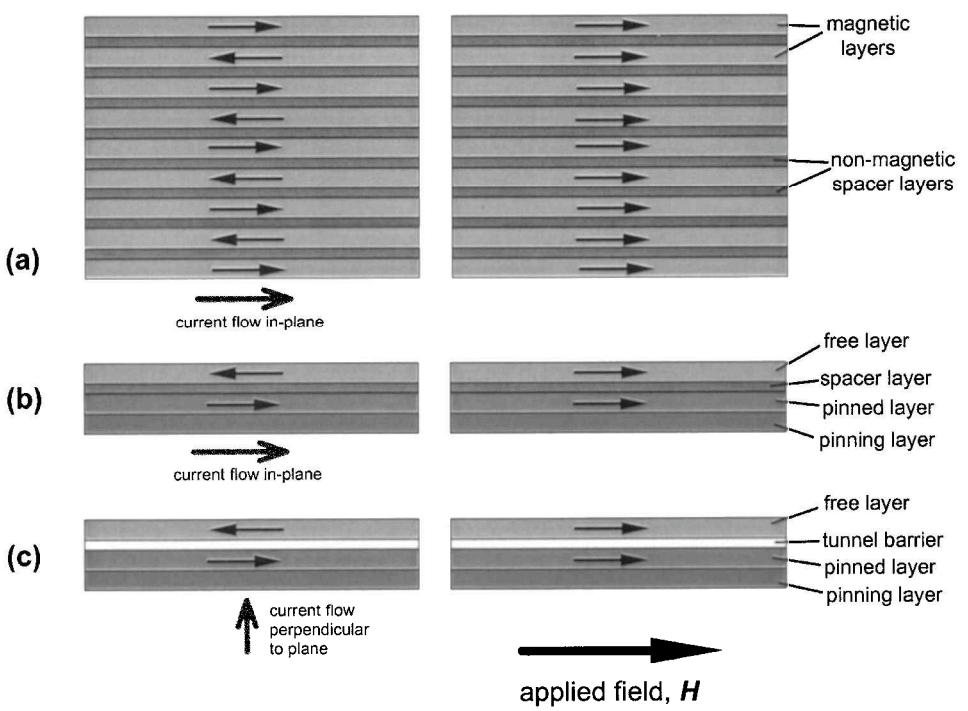

Figure 9. Layered structures for GMR sensors in high resistance state at zero field and low resistance state with a field applied: (*a*) multilayer, (*b*) spin valve and (*c*) spin tunnel junction.

direction and a 'free' layer in which the magnetization is free to rotate relative to the pinned layer when a field is applied. Thus high resistance (antiparallel) and low resistance (parallel) states can be achieved. Spin valves are already being used in GMR read heads where they provide good sensitivity to small fields from the media.

Spin tunnel junctions [63] have two magnetic electrodes separated by an insulating tunnel barrier made from aluminium oxide (figure 9(*c*)). Unlike in spin valves, the current flows through the junction perpendicular to the layers rather than in the plane of the layers. This increases the effect of the spin-dependent scattering on the electrons passing through the structure and leads to a higher $\Delta R/R$ of around 25%. In addition the higher resistance of spin tunnel junctions may be more suitable for low current applications.

4.2.3. *Design of the spin valve read head.* The use of GMR sensors in read heads for hard disks has been highly significant in the increase in storage density over the last few years. GMR sensors enable the detection of smaller fields from smaller bits. They also retain their properties better when scaled down in size than their predecessors, read heads based on the anisotropic magnetoresistance effect. A typical spin valve sensor element for a GMR read head is shown in figure 10. During operation of the hard disk system, the edge A–A′ of this layered structure passes over the tracks on the disk (compare figure 1). The layers in the spin valve are usually constructed so that in the rest state, with no signal being detected, the magnetization directions in the pinned and free layers are at right angles. $\mathbf{M}_p$ in the pinned layer lies across the stripe and $\mathbf{M}_f$ in the free layer lies parallel to the stripe. This gives a linear, bipolar response to applied field as the magnetization in the free layer swings either up or down depending on the orientation of the field detected. The magnetization in the pinned layer is fixed by an under- or over-lying antiferromagnet, such as FeMn, InMn, TbCo or NiO [64].

A number of parameters affect the properties of a spin valve: the materials of the layers and their crystal structure, ferromagnetic coupling between the pinned and free layers through the non-magnetic spacer layer, the uniformity and thermal stability of the antiferromagnetic pinning layer, and the strength of the induced anisotropy in the free layer.

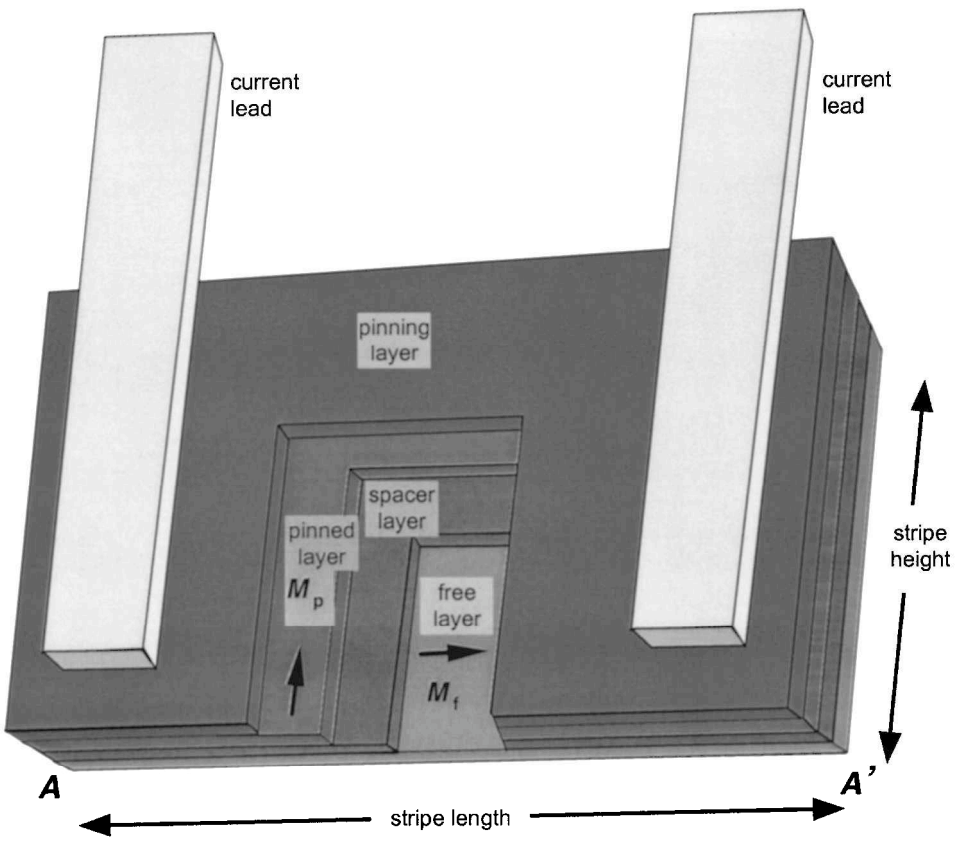

Figure 10. Cut-away diagram of magnetic layers in a spin valve read head showing orientation of magnetization in the free layer, $\mathbf{M}_f$, and the pinned layer, $\mathbf{M}_p$. In the rest state, with no field detected, $\mathbf{M}_f$ and $\mathbf{M}_p$ are at right angles. Stray field from the disk causes $\mathbf{M}_f$ to rotate, thus moving towards parallel or antiparallel alignment with $\mathbf{M}_p$.

Spin valves for read heads commonly have many extra layers to improve the performance of the device, including seed layers to promote textured growth of the film, a capping layer to protect the structure, and extra Co at the interfaces to enhance the GMR. The pinned layer is now likely to be a Co alloy rather than NiFe.

Ideally in a spin valve sensor, the magnetization in the pinned layer stays fixed and uniform whilst the magnetization in the free layer rotates uniformly under the influence of the external field. However in patterned elements of spin valve material, shape anisotropy in the individual layers and magnetostatic coupling between the magnetic layers, especially at the edges, will have significant effects. These magnetostatic effects become increasingly large as read heads are miniaturized so there is a strong tendency for their properties to be determined mainly by their shape. Shape effects may be strong enough to override the induced anisotropy in the free layer, the interlayer ferromagnetic coupling, and even the pinning of the pinned layer. This has been investigated by electrical measurements [65,66] and by micromagnetic simulations [67,68] . A simplified picture of these effects is given in figure 11. Proper bias, with $\mathbf{M}_f$ and $\mathbf{M}_p$ at right angles, is shown in figure 11 (*a*). As the dimensions of the spin valve element are reduced, the interaction caused by stray fields at the edges of the two magnetic layers tries to orient $\mathbf{M}_f$ to be antiparallel to the pinned layer as in figure 11 (*b*). For even narrower stripes, shape anisotropy in the pinned layer tries to rotate the $\mathbf{M}_p$ towards the long axis of the device, see figure 11 (*c*). A particular problem with the free layer is that demagnetizing effects tend to keep the magnetization at the edges of the stripe aligned parallel to the edge. Therefore it is less free to rotate and so less sensitive to the field from the disk.

Various techniques are in use to control the properties of the layers and avoid these problems. The correct alignment of the layers can be helped to some extent by using the field across the stripe, produced by the current through the sensor, to balance the other forces on the pinned layer. Bias magnets made from magnetically hard CoCrPt are often incorporated at the ends of the stripe to prevent domains forming in the free layer. To avoid the fields from the pinned layer acting to demagnetize the free layer, the pinned layer has been replaced by a laminated pinned layer, or 'artificial antiferromagnet', made from a Co–Ru–Co or a CoFe–Ru–CoFe trilayer [69,70]. The two Co layers are antiferromagnetically coupled so that their stray fields cancel out and do not affect the free layer. For the best properties, this composite layer must usually still be biased by an antiferromagnet.

The effects of patterning spin valves to micron dimensions can be seen in magnetic images from the transmission electron microscope [71]. Figure 12 shows shape effects on the reversal of the free layer for a 4 μm $\times$ 2 μm spin valve element. It is clear that reversal is not simply by uniform rotation but involves the formation of domains. The image at remanence (0 Oe) shows a complex flux closure domain pattern, and, in an applied field of 16 Oe opposite to the

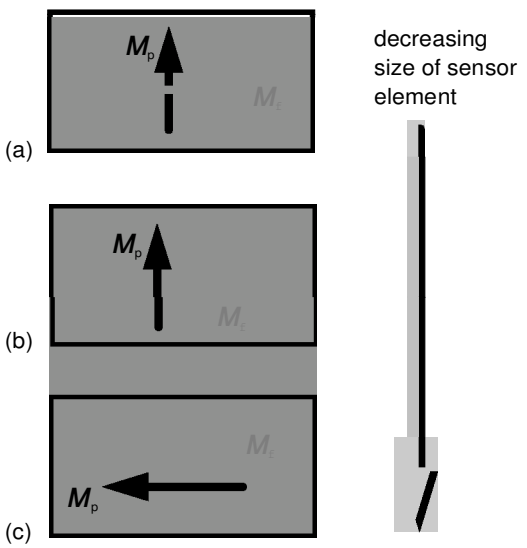

Figure 11. Simplified picture of the effect of decreasing the size of a spin valve sensor element: (*a*) proper bias, with the magnetization in the free and pinned layers at right angles; (*b*) interlayer magnetostatic interactions bring $\mathbf{M}_f$ into antiparallel alignment with $\mathbf{M}_p$; (*c*) shape anisotropy overcomes the pinning of the pinned layer, $\mathbf{M}_f$ is now aligned along the long axis, antiparallel to $\mathbf{M}_p$.

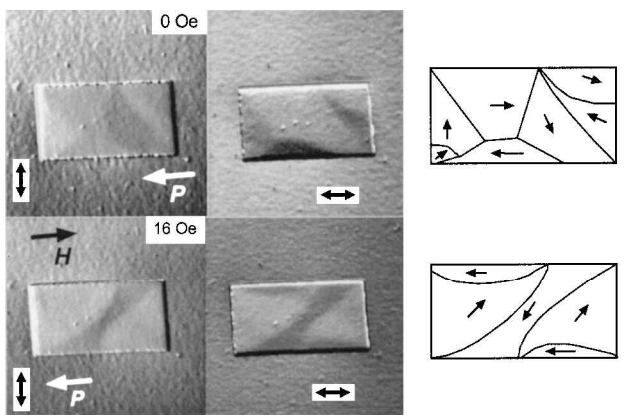

Figure 12. Magnetic images of spin valve element, 4 μm $\times$ 2 μm, during magnetization reversal of the free layer. H indicates the applied field direction, and P indicates the pinning direction. The complex domain structure is explained in the schematic diagrams. It is clear that reversal was not by uniform rotation of the free layer. The magnetization showed a strong tendency to align along the edges of the element. The layers in this spin valve structure were: 5 nm Ta (seed layer), 8 nm NiFe (free layer), 2.5 nm Cu (non-magnetic spacer layer), 6 nm NiFe (pinned layer), 6 nm FeMn (pinning layer), 5 nm Ta (capping layer).

pinning direction, we can see that domains at the edges seem to be resistant to reversal by the applied field **H**. This would result in a noisy, nonlinear signal and reduced sensitivity. Clearly deviations from simple rotation of $\mathbf{M}_f$ in the free layer caused by edge effects, rotation away from proper alignment, and loss of pinning all need to be addressed for further miniaturization of read heads.

4.3. *MRAM*

Magnetic memory elements are being developed as a new type of non-volatile random access memory (RAM) [72,73]. In certain applications magnetic RAM could replace silicon devices based on CMOS technology, and it has initially found a niche where resistance to radiation is important, for example, in satellites. It has been predicted that MRAM could have the density of DRAM (which is dense but relatively slow), and the speed of SRAM (which is fast but needs a large area on the chip to store one bit). Even better, MRAM retains the stored data when the power is switched off, so a computer using MRAM to store its operating system would not need time to boot up from the hard disk. The operation of magnetic memory cells is based on two of the magnetic phenomena discussed in this paper: the GMR effect in spin valves or spin tunnel junction structures and the special properties of nanomagnets as storage elements for binary data. As in patterned media (section 4.1), data can be stored because the nanomagnet has two stable states, but in MRAM the data is read by measuring the electrical resistance of the cell to distinguish between the two states. Thanks to GMR this signal is large enough to be useful for devices.

4.3.1. *Operation of a magnetic memory cell.* A typical magnetic memory cell has two magnetic layers (usually NiFe or NiFeCo, <10 nm thick) separated by a non-magnetic spacer. Data is written by changing the orientation of one of the magnetic layers in the cell using the field generated by a current passing through thin film wires above and below the cell. Nanomagnets for MRAM tend to be low aspect ratio rectangular elements with the length about twice the width. They are elongated just enough for shape anisotropy to impose an easy axis and produce two stable magnetization states. As in the elongated elements considered previously for patterned media, magnetization reversal is likely to start from domain structures at the ends of the elements. However the ends are now close enough together for the end domains to interact during switching. Therefore the exact reversal process has a significant effect on the switching field.

As with GMR sensors it is necessary to have some way of switching just one of the magnetic layers, relative to the other, and several schemes have been proposed to achieve this. In the pseudo spin valve one of the magnetic layers is thicker than the other and therefore has a higher switching field [74]. The data is stored by the orientation of magnetization in the thicker 'hard' layer (figure 13 (*a*)). To read the data a smaller field pulse is used to flip the magnetization in the thinner 'soft' layer first one way and then the other. Comparing the resistance measured in each direction reveals the orientation of the magnetization in the storage layer. Another method is to use a spin valve structure in which the free layer is switched relative to the pinned layer to store a 0 or a 1 (figure 13 (*b*)). Measuring the resistance of the element indicates its magnetic state. These are both non-destructive readout schemes, because the data remains intact whilst it is being read, unlike in DRAM. Spin tunnel junctions, with higher GMR and higher resistance are most likely to be suitable for MRAM [72]. They

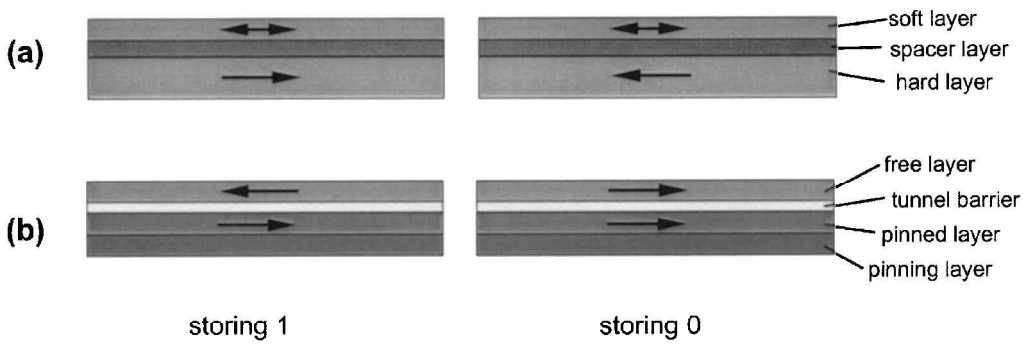

Figure 13. Data storage in MRAM memory cells. In the pseudo spin valve memory cell (*a*), data is stored in the magnetization direction of the thicker 'hard' layer. The data is read by switching the magnetization direction in the thinner 'soft' layer from one direction to the other and comparing the resistance values. In the spin valve memory cell (*b*), data is stored by having the free layer either parallel or antiparallel to the pinned layer, giving either low or high resistance for the cell. Metallic spacer layers or insulating tunnel barriers could be used for either type of MRAM cell.

could be incorporated into either pseudo spin valve or spin valve type structures.

In order to achieve high density memory it helps greatly if there is a simple method to select a single cell for reading or writing, without having extra components such as transistors at each memory location. For MRAM using a metal spacer layer, simple matrix addressing is possible in which a cell is selected by the combined field from the word line passing above the cell, electrically isolated from it, and the sense line which connects the cells together in series. The two current lines cross at right angles and produce two field components. H_w, due to the word line is directed along the switching direction. H_s, a smaller field from the sense line, is perpendicular to the switching direction and assists in the rotation of the magnetization during switching. Only the cell at the intersection is selected, the other cells in each row or column only receive one component of the field and do not switch. If coherent rotation can be assumed H_w and H_s will correspond to H_{easy} and H_{hard} in the Stoner–Wohlfarth model (9) so methods based on the Stoner–Wohlfarth approach have been used to help predict the components of field required for switching [75]. Similar considerations apply for tunnel junctions, but in this case two write current lines are used crossing at right angles and insulated from the cell. Since in a tunnel junction the sense current has to flow perpendicular to the layers, additional components (one diode per cell) are needed to prevent unwanted current paths through an array of memory cells.

4.3.2. *Domain processes and switching.* It is important that nanomagnets for MRAM cells have repeatable and consistent switching behaviour and the shape of the elements has turned out to be very important for this. Experiments on simple rectangular elements have shown them to have an unacceptably large variation in switching field [74]. This is thought to be because the reversal processes tend to be more unpredictable in rectangular elements where so many different domain patterns are allowed by symmetry. For example, consider a simple domain structure in a rectangular element consisting of a single main domain plus the small end domains which form to lower the magnetostatic energy by reducing the stray field (figure 14). There are two possibilities, both equally likely to occur. In the S-state (figure 14 (*a*)) the end domains are magnetized in the same direction whilst in the C-state (figure 14 (*b*)) they are oppositely magnetized. Micromagnetic modelling predicts the two states to have different switching fields of 74 Oe for the S-state and 86 Oe for the C-state, for Co elements 0.5 μm $\times$0.25 μm $\times$1.5 nm [76]. Switching is evidently facilitated in the S-state when the end domains are magnetized the same way and can more easily amalgamate during switching.

The effect of the geometry of an element has been investigated by modelling and experiments in order to obtain improved switching performance and repeatability. Pointed and elliptical ends have been studied by magnetic imaging in the TEM [35]. Figure 15 shows that, for NiFe nanomagnets 41 nm thick, end domains formed at rectangular (*a*) and blunt elliptical ends (*b*), but not at sharper elliptical (*c*) or pointed ends (*d*). Simulations of thinner NiFe elements showed both elliptical and pointed ends reversing mainly by rotation, without the formation of domains [77].

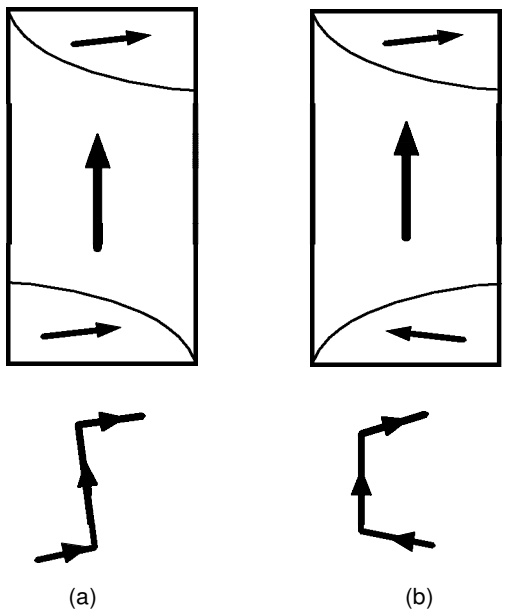

Figure 14. Two possible domain structures for MRAM elements with 2 : 1 aspect ratio. In the S-state (*a*) the end domains point the same direction and in the C-state (*b*) they point in opposite directions. For a Co element 0.5 μm $\times$0.25 μm $\times$1.5 nm, the switching fields were calculated to be 74 Oe for the S-state and 86 Oe for the C-state [76].

It has already been noted that suppressing the formation of domains at the ends of nanomagnets raises their switching field [39]. This is a problem for MRAM because switching fields need to be low to fall within the range which can be generated using thin film current lines carrying 20–30 mA. The target is therefore for rather low switching fields of $<$100 Oe, which could perhaps be achieved using thinner films with transverse anisotropy. Since the behaviour of MRAM cells depends crucially on the properties of nanomagnets, they should perform well when miniaturized further, especially since they will increasingly closely approach a single domain state. However it will be difficult to achieve very low switching fields as the element width is reduced. Issues of stability over millions of magnetization reversal cycles [78] and device noise, in particular 1/*f* noise generated in the tunnel barrier [79], are also under investigation.

Magnetic memory chips will of course need very short read and write times for rapid access to the data. Dynamic simulations and high speed experiments have therefore been used to investigate the effect of using very short duration pulses for switching. In experiments by Russek *et al*. [80] switching times of a few tenths of a nanosecond were obtained in a spin valve element 0.6 μm wide. The switching field was found to increase as the inverse of the pulse width for pulses in the range 0.5–10 ns. In simulations of high-speed switching in spin tunnel junction structures, 0.8 μm $\times$ 1.6 μm, mechanisms of magnetization reversal have been predicted which differ from those seen in samples switched at low speeds [81]. The simulations showed there was a tendency for the magnetization to be pinned at the edges of a magnetic element, whilst the central region rotated more freely. Experimental results for the magnetization in the free layer agreed well with the predictions from the dynamic model. For example, a 200 ps field pulse produced oscillations in the average magnetization with a period of 0.5–1.0 ns depending on the strength of the field.

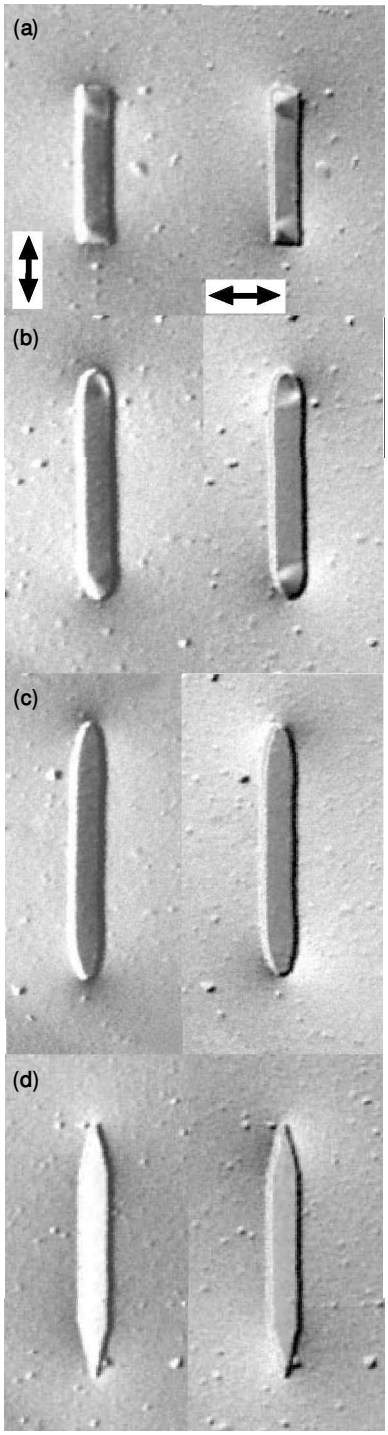

Figure 15. Magnetic images of the effect of end shape on the domain structure in NiFe nanomagnets 300 nm wide and 41 nm thick. Domains form at rectangular ends (*a*) and blunt elliptical ends (*b*), but not at sharper elliptical ends (*c*) or pointed ends (*d*). Shading indicates magnetization directions, mapped parallel to the arrows. Stray fields can be seen clearly outside the elements.

5. Future prospects in nanomagnetics

Spin valves are now well established as the sensor elements in read heads for hard disks and spin tunnel junctions may follow [82]. Much work is continuing in materials research and device design to improve and develop their properties. Important issues to be resolved for spin tunnel junctions are how to lower the very high resistance, reduce the noise, and cope with the increased danger of damage by electrostatic discharge. Further improvements required for spin valve sensors are greater uniformity of pinning and better high temperature stability. The high temperature performance is important for rugged sensors in high temperature applications (bearing in mind that an ordinary read head operates at 125–150°C) and also to ensure sensors can survive some high temperature processing when incorporated into integrated semiconductor circuits.

New devices are being devised in the field of spin electronics [83,84] such as spin transistors and hybrid magnetic and semiconductor devices. Metallic devices based on the spin of the electron could be miniaturized to much smaller sizes than semiconductor devices before running into problems associated with having too few electrons in the device. However a useful transistor has not yet been produced.

Colossal magnetoresistance (CMR) materials have extremely large magnetoresistance ratios of $>100\%$. The most widely studied group of CMR materials are calcium-doped lanthanum manganese oxides, $La_{1-x}Ca_xMnO_3$, which form a perovskite crystal structure [85]. CMR materials are still some way from commercial exploitation because initially the best results were obtained at cryogenic temperatures, using fields of several Tesla, and at normal temperatures the effect had disappeared. However recent reports are more promising, with room temperature

operation now possible and lower saturation fields being achieved using ceramic materials, tunnel junction structures, or artificial grain boundaries grown on bi-crystal $SrTiO_3$ substrates [86].

Further miniaturization of magnetic devices requires high resolution fabrication. It has been exciting to see the developments in mechanical pattern transfer, enabling features down to a few tens of nanometres to be produced by imprinting or moulding. It should also be noted that the smallest dimensions attainable using optical lithography are now firmly in the 100–200 nm regime.

High resolution magnetic imaging is already possible using electron microscopy methods. Magnetic force microscopy and near-field magneto-optical techniques are improving in resolution and ease of interpretation. Comparison of these experimental images with computed magnetization distributions is helping in the development of more reliable micromagnetic simulations. Magnetic imaging with fast time resolution would help in understanding the high speed processes occurring in real devices. To date spatial distribution of high speed magnetic processes has been seen in an 8 μm NiFe disk using time resolved scanning Kerr effect microscopy [87]. Near-field optical techniques will be necessary to increase the spatial resolution.

It is clear that nanomagnets are hugely important for many important devices and systems in use today. In particular they provide the major form of data storage during a time when our requirement for storage capacity show no sign of diminishing. The advent of GMR together with other developing technologies, will ensure that nanomagnets continue to expand their role at the same time as we shrink their dimensions.

Acknowledgements

I would like to thank Professor J. N. Chapman for his helpful comments on my initial draft of this paper. I would also like to acknowledge the contribution of Professor Chapman, Dr S. McVitie, Dr P. R. Aitchison and Professor C. D. W. Wilkinson to the work at Glasgow described here.

References

[1] Raia, E., 1999, *Data Storage,* **January,** 5.
[2] 1995, *Magnetoelectronics Special Issue, Phys. Today,* **48**(4).
[3] Prinz, G. A., 1998, *Science,* **282,** 1660.
[4] Jiles, D., 1991, *Introduction to Magnetism and Magnetic Materials* (London: Chapman and Hall), chap. 4, pp. 69–81.
[5] Baibich, M. N., Broto, J. M., Fert, A., Vandau, F. N., Petroff, F., Eitenne, P., Creuzet, G., Friederich, A., and Chazelas, J. J. N., 1999 *Phys. Rev. Lett.,* **61,** 2472.
[6] Daughton, J., 1999, *J. Magn. Magn. Mater.,* **192,** 334.
[7] Wolf, S., 1999, presented at the *MRS Spring Meeting*, 5–8 April; see also DARPA web site at http://www.darpa.mil/dso/rd/materials/magnetic.html.
[8] de Boeck, J., and Borghs, G., 1999, *Phys. World,* **April,** 27.
[9] Lodder, J. C., 1995, *MRS Bull.,* **October,** 59.
[10] Suzuki, T., 1996, *MRS Bull.,* **September,** 42.
[11] Takagi, A., 1997, *Data Storage,* **May/June,** 47.
[12] Betzig, E., Trautman, J. K., Wolfe, R., Gyorgy, E. M., Finn, P. L., Kryder, M. H., and Chang, C. H., 1992, *Appl. Phys. Lett.,* **61,** 142.
[13] Knight, G., 1998, *Data Storage,* **February,** 23.
[14] Raia, E., 1999, *Data Storage,* **March,** 10.
[15] 1995, *Magnetisation on a Microscopic Scale Special Issue, MRS Bull.,* **20** (10).
[16] Miramond, C., Fermon, C., Rousseaux, F., and Decanini, D., 1997, *J. Magn. Magn. Mater.,* **165,** 500.
[17] Savas, T. A., Farhoud, M., Hwang, M., Smith, H. I., and Ross, C. A., 1999, *J. Appl. Phys.,* **85,** 6160.
[18] Teichert, C., Barthel, J., Oepen, H. P., and Kirshner, J., 1999, *Appl. Phys. Lett.,* **74,** 588.
[19] Fasol, G., 1998, *Science,* **280,** 545.
[20] Palacin, S., Hidber, P. C., Bourgoin, J.-Ph., Miramond, C., Fermon, C., and Whitesides, G. M., 1996, *Chem. Mater.,* **8,** 1316.
[21] Wu, W., Cui, B., Sun, X., Zhang, W., Zhuang, L., Kong, L., and Chou, S. Y., 1998, *J. vac. Sci. Technol.,* **B16,** 3825.
[22] Hubert, A., and Schäfer, R., 1998, *Magnetic Domains: The Analysis of Magnetic Microstructures* (Berlin, Heidelberg: Springer-Verlag), chap. 2, pp. 11–106.
[23] Chapman, J. N., 1984, *J. Phys. D: Appl. Phys.,* **17,** 623.
[24] Chapman, J. N., and Kirk, K. J., 1997, *Magnetic Hysteresis in Novel Magnetic Materials*, edited by G. Hadjipanayis (Amsterdam: Kluwer Academic Publishers), pp. 195–206.
[25] New, R. M. H., Pease, R. F. W., White, R. L., Osgood, R. M., and Babcock, K., 1996, *J. Appl. Phys.,* **79,** 5851.
[26] Fernandez, A., Bedrossian, P. J., Baker, S. L., Vernon, S. P., and Kania, D. R., 1996, *IEEE Trans. Magn.,* **32,** 4472.
[27] Hehn, M., Ounadjela, K., Bucher, J. P., Rousseaux, F., Decanini, D., Bartenlian, B., and Chappert, C., 1996, *Science,* **272,** 1782.
[28] Gomez, R. D., Burke, E. R., and Mayergoyz, I. D., 1996, *J. Appl. Phys.,* **79,** 6441.
[29] Wirth, S., Heremans, J. J., von Molnar, S., Field, M., Campman, K. L., Gossard, A. C., and Awschalom, D. D., 1998, *IEEE Trans. Magn.,* **34,** 1105.
[30] Luo, Y., and Zhu, J. G., 1994, *IEEE Trans. Magn.,* **30,** 4080.
[31] Wernsdorfer, W., Doudin, B., Mailly, D., Hasselbach, K., Benoit, A., Meier, J., Ansermet, J.-Ph., and Barbara, B., 1996, *Phys. Rev. Lett.,* **77,** 1873.
[32] O'Barr, R., and Schultz, S., 1997, *J. Appl. Phys.,* **81,** 5458.
[33] Cros, V., Lee, S. F., Faini, G., Cornette, A., Hamzic, A., and Fert, A., 1997, *J. Magn. Magn. Mater.,* **165,** 512.
[34] McVitie, S., and Chapman, J. N., 1988, *IEEE Trans. Magn.,* **24,** 1778.
[35] Kirk, K. J., Chapman, J. N., and Wilkinson, C. D. W., 1999, *J. Appl. Phys.,* **85,** 5237.
[36] Hubert, A., and Schäfer, R., 1998, *Magnetic Domains: The Analysis of Magnetic Microstructures* (Berlin, Heidelberg: Springer-Verlag), chap. 3, pp. 238–271.
[37] Ramstöck, K., Hartung, W., and Hubert, A., 1996, *Phys. status solidi (a),* **155,** 505.
[38] Rührig, M. R., Khamsehpour, B., Kirk, K. J., Chapman, J. N., Aitchison, P. R., McVitie, S., and Wilkinson, C. D. W., 1996, *IEEE Trans. Magn.,* **32,** 4452.
[39] Kirk, K. J., Chapman, J. N., and Wilkinson, C. D. W., 1997, *Appl. Phys. Lett.,* **71,** 539.
[40] Hubert, A., and Schäfer, R., 1998, *Magnetic Domains: The Analysis of Magnetic Microstructures* (Berlin Heidelberg: Springer-Verlag), chap. 3, p. 155.
[41] Chikazumi, S., 1964, *The Physics of Magnetism,* English edition, edited by S. H. Charap (New York, Chichester: John Wiley and Sons), chap. 2, p. 21.

[42] Awschalom, D. D., and DiVincenzo, D. P., 1995, *Phys. Today,* **April,** 43.
[43] Schrefl, T., 1997, *Magnetic Hysteresis in Novel Magnetic Materials*, edited by G. Hadjipanayis (Amsterdam: Kluwer Academic Publishers), pp. 49–68.
[44] Weller, D., and Moser, A., *IEEE Trans. Magn.* (in the press).
[45] Chou S. Y., Wei, M. S., Krauss, P. R., and Fischer, P. B., 1994, *J. Appl. Phys.,* **76,** 6673.
[46] Charap, S. H., Lu, P. L., and He, Y., 1997, *IEEE Trans. Magn.,* **33,** 978.
[47] Grundy, P. J., 1998, *J. Phys. D: Appl. Phys.,* **31,** 2975.
[48] Xiong, W., and Hoo, H. L., 1998, *Data Storage,* **July/August,** 47.
[49] Chou, S. Y., Krauss, P. R., and Kong, L., 1996, *J. Appl. Phys.,* **79,** 6101.
[50] Kong, L., Shi, R. C., Krauss, P. R., and Chou, S. Y., 1997, *Jpn. J. Appl. Phys.,* **36,** 5109.
[51] Wong, J., Scherer, A., Todorovic, M., and Schultz, S., 1999, *J. Appl. Phys.,* **85,** 5489.
[52] Ross, C. A., and Smith, H. I., 1998, *Data Storage,* **September,** 41.
[53] Chou, S. Y., Krauss, P. R., Zhang, W., Guo, L., and Zhuang, L., 1997, *J. Vac. Sci. Technol.,* **B15,** 2897.
[54] Casey, B. G., Monaghan, W., and Wilkinson, C. D. W., 1997, *Microelectron. Eng.,* **35,** 393.
[55] Brittain, S., Paul, K., Zhao, X. M., and Whitesides, G., 1998, *Phys. World,* **May,** 31.
[56] Chappert, C., Bernas, H., Ferre, J., Kottler, V., Jamet, J. P., Chen, Y., Cambril, E., Devolder, T., Rousseaux, F., Mathet, V., and Launois, H., 1998, *Science,* **280,** 1919.
[57] Speliotis, D., 1999, *Data Storage,* **January,** 25.
[58] Barthelemy, A., Fert, A., Morel, R., and Steren, L., 1994, *Phys. World,* **November,** 34.
[59] Parkin, S. S. P., Li, Z. G., and Smith, D. J., 1991, *Appl. Phys. Lett.,* **58,** 2710.
[60] Highmore, R. J., Blamire, M. G., Somekh, R. E., and Evetts, J. E., 1992, *J. Magn. Magn. Mater.,* **104,** 1777.
[61] Kubinski, D. J., and Holloway, H., 1996, *J. Appl. Phys.,* **79,** 1661.
[62] Dieny, B., Speriosu, V., Metin, S., Parkin, S. S. P., Gurney, B. A., Baumgart, P., and Wilhoit, D. R., 1991, *J. Appl. Phys.,* **69,** 4774.
[63] Moodera, J. S., Kinder, L. R., Wong, T. M., and Meservey, R., 1995, *Phys. Rev. Lett.,* **74,** 3273.
[64] Kools, J. C. S., 1996, *IEEE Trans. Magn.,* **32,** 3165.
[65] Cross, R. W., Kim, Y. K., Oti, J. O., and Russek, S. E., 1996, *Appl. Phys. Lett.,* **69,** 3935.
[66] Lu, Y., Altman, R. A., Marley, A., Rishton, S. A., Troulliard, P. L., Xiao, G., Gallagher, W. J., and Parkin, S. S. P., 1997, *Appl. Phys. Lett.,* **70,** 2610.
[67] Oti, J. O., Cross, R. W., and Russek, S. E., 1996, *J. Appl. Phys.,* **79,** 6386.
[68] Yuan, S. W., and Bertram, H. N., 1994, *J. Appl. Phys.,* **75,** 6385.
[69] van den Berg, H. A. M., Clemens, W., Gieres, G., Rupp, G., Schelter, W., and Vieth, M., 1996, *IEEE Trans. Magn.,* **32,** 4624.
[70] Huai, Y., Zhang, J., Anderson, G. W., Rana, P., Funada, S., Hung, C. Y., Zhao, M., and Tran, S., 1999, *J. Appl. Phys.,* **85,** 5528.
[71] Chapman, J. N., Aitchison, P. R., Kirk, K. J., McVitie, S., Kools, J. C. S., and Gillies, M. F., 1998, *J. Appl. Phys.,* **83,** 5321.
[72] Parkin, S. S. P., Roche, K. P., Samant, M. G., Rice, P. M., Beyers, R. B., Scheuerlein, R. E., O'Sullivan, E. J., Brown, S. L., Bucchigano, J., Abraham, D. W., Lu, Y., Rooks, M., Trouillard, P. M., Wanner, R. A., and Gallagher, W. J., 1999, *J. Appl. Phys.,* **85,** 5828.
[73] Tehrani, S., Chen, E., Durlam, M., DeHerrera, M., Slaughter, J. M., Shi, J., and Kerszykowski, G., 1999, *J. Appl. Phys.,* **85,** 5822.
[74] Everitt, B. A., Pohm, A. V., Beech, R. S., Fink, A., and Daughton, J. M., 1998, *IEEE Trans. Magn.,* **34,** 1060.
[75] Everitt, B. A., Pohm, A. V., and Daughton, J. M., 1997, *J. Appl. Phys.,* **81,** 4020.
[76] Zheng, Y., and Zhu, J. G., 1997, *J. Appl. Phys.,* **81,** 5471.
[77] Gadbois, J., Zhu, J. G., Vavra, W., and Hurst, A., 1998, *IEEE Trans. Magn.,* **34,** 1066.
[78] Gider, S., Runge, B. U., Marley, A. C., and Parkin, S. S. P., 1998, *Science,* **281,** 797.
[79] Nowak, E. R., Weissman, M. B., and Parkin, S. S. P., 1999, *Appl. Phys. Lett.,* **74,** 600.
[80] Russek, S. E., Oti, J. O., Kaka, S., and Chen, E. Y., 1999, *J. Appl. Phys.,* **85,** 4773.
[81] Koch, R., Deak, J. G., Abraham, D. W., Trouillard, P. L., Altman, R. A., Lu, Y., Gallagher, W. J., Scheuerlein, R. E., Roche, K. P., and Parkin, S. S. P., 1998, *Phys. Rev. Lett.,* **81,** 4512.
[82] Zhang, J., 1998, *Data Storage,* **November,** 31.
[83] Gregg, J., Allen, W., Viart, N., Kirschman, R., Sirisathitkul, C., Schille, J.-P., Gester, M., Thompson, S., Sparks, P., Da Costa, V., Ounadjela, K., and Skvarla, M., 1997, *J. Magn. Magn. Mater.,* **175,** 1.
[84] Prinz, G. A., 1995, *Phys. Today,* **April,** 58.
[85] Sun, J. Z., Krusin-Elbaum, L., Gupta, A., Xiao, G., Duncombe, P. R., and Parkin, S. S. P., 1998, *IBM J. Res. Develop.,* **42,** 89.
[86] Fontcuberta, J., 1999, *Phys. World,* **February,** 33.
[87] Hiebert, W. K., Stankiewicz, A., and Freeman, M. R., 1997, *Phys. Rev. Lett.,* **79,** 1135.

Katherine Kirk is a postdoctoral researcher at Glasgow University. She has been investigating nano-magnetic structures and devices for 4 years. This involves fabricating thin film magnetic elements using high resolution techiques and studying how their magnetic properties are affected. Katherine received a degree in physics from Manchester University, where she first became interested in thin films. This was followed by a PhD in physics at Strathclyde University on the proximity effect in high temperature superconductors. After her PhD she worked on high temperature ultrasonic transducers for non-destructive testing, also at Strathclyde University. She then began work at Glasgow University on her current project, which combines magnetic imaging in the transmission electron microscope in the Department of Physics and Astronomy and nanofabrication in the Department of Electronics and Electrical Engineering.